Modeling of Generalized Coaxial Probes in Rectangular Waveguides

Hui-Wen Yao, *Student Member, IEEE*, and Kawthar A. Zaki, *Fellow, IEEE*

***Abstract*—A rigorous approach combining the orthogonal expansion method for modeling cylindrical posts in rectangular waveguides and the extension of the three short plane technique is introduced to obtain the S-matrix for a general coaxial probe in a rectangular waveguide. A cascading procedure is applied to solve the problem of a probe near a waveguide discontinuity and to obtain the response of a probe-excited band pass filter. The computed results are in excellent agreement with the measured results showing the usefulness of this method.**

I. Introduction

An IMPORTANT problem in many microwave applications is to characterize coaxial probes in rectangular waveguides. Two commonly encountered configurations are coaxial line-waveguide T-junctions and coaxial line-waveguide transitions (coaxial probe excited semi-infinite waveguides). The two configurations are closely related.

Over the years, considerable effort has been made to solve the problems [1]–[5], [18]. In analysis in [1], a variational method is used to obtain the expression of input impedance for a coaxial probe in a rectangular waveguide by assuming a single modal current located at the center of the probe. This assumption leads to inaccurate results for a thick probe. Using multifilament current approximation in the method of moment, [3] improves the accuracy of impedance computation and shows that the probe surface current has significant azimuthal variation. However, [3] neglects the effect of the end surface of the probe. In [2], an image theory is employed to develop a closed form expression of input admittance for a hollow probe in rectangular waveguide. A dielectric coated probe in waveguide is studied in [4] and [5]. A disc-ended probe is studied in [18] by a field matching method. Similar to [1], the work in [2], [4], [5], and [18] is based on the assumption that the current (or field) on the surface of the probe is uniform in angular distribution. Besides, all the above analyses were focused on computing the input impedance (admittance) of a coaxial probe in a rectangular waveguide. However, in many applications, for instance, in designs of probe excited cavity filters and coax-waveguide T-junction manifold multiplexers, it is essential to have the S-parameters of the transitions and the T-junctions. In particular, in the case of a probe located in a section of evanescent mode waveguide, such as a probe excited evanescent mode cavity filter, or a probe near a waveguide discontinuity, it is necessary to know the generalized S-parameters of the coaxial probe in the waveguide in order to design the probe accurately. Limited investigation has been published for such cases. In [6], two-port S-parameters of a coaxial line to waveguide transition is analyzed by three cavity moment method assuming one propagating mode in both the waveguide and the coaxial line. This analysis is valid for a thin probe with simple shape and is incapable of computing generalized S-parameters.

Recently, the orthogonal expansion method has been successfully applied to solve the scattering by dielectric cylindrical posts in rectangular waveguide [7]–[9]. Similar method is also used in [10]. This method provides the generalized scattering matrix and yields very reliable and accurate results. Since the cylindrical post region is treated separately, the method is flexible.

In this paper, a new approach, which combines the orthogonal expansion method and the extension of the three short plane technique [11]–[13], is introduced to model the generalized S-parameters for more general structures of coax-waveguide T-junctions and transitions. The generalized S-parameters are obtained for all the higher-order modes present in rectangular waveguides, but only for dominant mode in coaxial lines. Theoretically, there is no approximations in the method and no limitations on the thickness of the probe. The convergence of the numerical solutions is tested. the correctness of the results is confirmed by comparing the computed results with the measurements. As an application of the modeling, a probe-excited dielectric block filter is analyzed, the simulated response is in good agreement with the measured one.

II. Modeling Procedure

The configuration under consideration is shown in Fig. 1, in which a disc loaded probe coated with a layer of dielectric in a rectangular waveguide is excited by a coaxial line. When both sides of the rectangular waveguide extend to infinity, one has a coax-waveguide T-junction. If one of the two waveguide ports is shorted at some place, the configuration represents a coax-waveguide transition. This configuration covers the most practical structures of coaxial probes in rectangular waveguides.

Modeling of the T-junction (transition) involves the following steps: solving the generalized S-parameters of the two-port network (one-port network) when the coaxial port of the T-junction (transition) is shorted at certain place, and extracting the three-port (two-port) generalized S-parameters from the obtained two-port (one-port) S-matrices. When a waveguide discontinuity is presented very close to a coaxial probe, a special cascading algorithm using S-matrices can be applied to solve the whole problem.

Manuscript received February 27, 1995; revised July 10, 1995.
The authors are with the Department of Electrical Engineering, University of Maryland, College Park, MD 20742 USA.
IEEE Log Number 9415478.

0018–9480/95$04.00 © 1995 IEEE

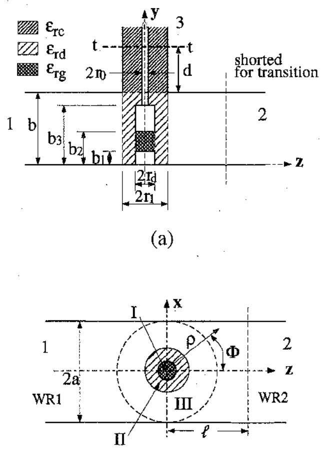

Fig. 1. Configuration of a general coaxial probe in a rectangular waveguide with (a) cross section view, and (b) top view.

A. Modeling of General Cylindrical Post in Rectangular Waveguide

When the coaxial port of the T-junction is shorted at the position t-t (Fig. 1), the structure can be viewed as a general cylindrical post in a rectangular waveguide. To apply the orthogonal expansion method [7]–[9], the resulting two-port network is divided into waveguide region "WR" and post interaction region "PR" by introducing an artificial cylindrical boundary at $\rho = a$. The post interaction region can be further divided into subregions according to the natural cylindrical boundaries of the geometry. In the case $r_d \leq r_1$, the subregions are: region I which consists of region I_1 ($\rho < r_d$, $b_1 \leq y < b_2$) and region I_2 ($r_0 \leq \rho < r_d$, $b_3 \leq y < b + d$), region II ($r_d \leq \rho < r_1$, $0 \leq y < b + d$), and region III ($r_1 \leq \rho < a$, $0 \leq y < b$). Each of these cylindrical regions can be treated as a multilayer parallel plane bounded in y-direction in which the eigenvalues and the eigenfunctions can be solved in close forms [14]. Then, similar to [19], the boundary conditions on all the natural cylindrical boundaries are forced to be satisfied. By taking cross inner product to the electric field continuity equations with the magnetic fields of the eigenmodes at the region with larger effective nonconducting surface and to the magnetic continuity equations with the electric fields of the eigenmodes at the region with smaller nonconducting surface, one may finally obtain a matrix equation in the form

$$[[M_C^{\text{III}}]\ [M_D^{\text{III}}]]\begin{bmatrix}\mathbf{C}^{\text{III}}\\ \mathbf{D}^{\text{III}}\end{bmatrix} = 0 \tag{1}$$

where $\mathbf{C}^{\text{III}}$ and $\mathbf{D}^{\text{III}}$, vectors of size N^{III} (N^{III} represents the number of eigenmodes used in region III), are the field coefficients of the eigenmodes in region III related to the outer-going and the inner-going cylindrical waves, respectively. $[M_C^{\text{III}}]$ and $[M_D^{\text{III}}]$, matrices of size $N^{\text{III}} \times N^{\text{III}}$, can be grouped as diagonal block matrices in terms of ϕ variations since the eigenmodes with different ϕ variations are decoupled. This factor can be used to improve the efficiency of matrix operations.

The fields in waveguide regions are related to the fields in region III by applying boundary conditions at the artificial boundary. Taking proper inner products to the field continuity equations using both E and H fields of the eigenmodes in region III, the following equations may be obtained [19]

$$\begin{bmatrix}\mathbf{C}^{\text{III}}\\ \mathbf{D}^{\text{III}}\end{bmatrix} = \begin{bmatrix}[M_A^{11}] & [M_A^{12}]\\ [M_A^{21}] & [M_A^{22}]\end{bmatrix}\begin{bmatrix}\mathbf{A}^{(1)}\\ \mathbf{A}^{(2)}\end{bmatrix} + \begin{bmatrix}[M_B^{11}] & [M_B^{12}]\\ [M_B^{21}] & [M_B^{22}]\end{bmatrix}\begin{bmatrix}\mathbf{B}^{(1)}\\ \mathbf{B}^{(2)}\end{bmatrix} \tag{2}$$

where $\mathbf{A}^{(i)}$ and $\mathbf{B}^{(i)}$ are vectors of size $N_W^{(i)}$, representing the field coefficients of the incident and reflected waves in waveguide 'i' ($i = 1$, or 2), respectively. $N_W^{(i)}$ is the number of modes used in waveguide 'i'. The elements of the sparse matrices $[M_A]$ and $[M_B]$ are determined by the inner products.

From (1) and (2), the generalized scattering matrix $[S^{t\text{-}t}]$ of the general cylindrical post in a rectangular waveguide can be acquired as

$$\begin{bmatrix}\mathbf{B}^{(1)}\\ \mathbf{B}^{(2)}\end{bmatrix} = \begin{bmatrix}[S_{11}^{t\text{-}t}] & [S_{12}^{t\text{-}t}]\\ [S_{21}^{t\text{-}t}] & [S_{22}^{t\text{-}t}]\end{bmatrix}\begin{bmatrix}\mathbf{A}^{(1)}\\ \mathbf{A}^{(2)}\end{bmatrix} = [S^{t\text{-}t}]\begin{bmatrix}\mathbf{A}^{(1)}\\ \mathbf{A}^{(2)}\end{bmatrix} \tag{3}$$

where the superscript 't-t' refers to the short plane t-t.

Equation (3) can be obtained only under the condition of $N^{\text{III}} = N_W^{(1)} + N_W^{(2)}$, that is, the number of modes used in region III must be equal to the total number of modes used in both sides of the waveguide. In order to avoid singular matrix when matching the artificial boundary, the eigenmodes used in both region III and the waveguide regions have to be selected carefully. The general rule of selecting the modes is: the numbers of the modes with same y-variations in region III and in the waveguide regions must be equal. For the case of PMC at the $x = 0$ plane, one possible selection of the modes is: Waveguide region 1 and 2

$$\text{TE}_{ij} \quad i = 1, 3, \ldots N_x, \quad j = 0, 1, 2, \ldots N_y;$$

and

$$\text{TM}_{ij} \quad i = 1, 3, \ldots N_x, \quad j = 1, 2, \ldots N_y;$$

Cylindrical region III

$$(\text{TE}_y)_{ij} \quad i = 1, 2, \ldots (N_x + 1), \quad j = 1, 2, \ldots N_y;$$

and

$$(\text{TM}_y)_{ij} \quad i = 0, 1, 2, \ldots N_x, \quad j = 0, 1, 2, \ldots N_y$$

where N_x (odd) and N_y are maximum indexes of the modes used in waveguide regions. The numbers of the modes used in the other cylindrical regions can be determined according to the ratio of the height of the regions to that of region III in order to have better convergence of numerical solutions [15], [16].

If port 2 of the waveguide is shorted at the distance ℓ from the center of the probe, the short circuit condition $\mathbf{A}^{(2)} = [\Lambda]\mathbf{B}^{(2)}$ can be applied to (3) to obtain

$$\mathbf{B}^{(1)} = [R^{t\text{-}t}]\mathbf{A}^{(1)} \tag{4}$$

$$[R^{t\text{-}t}] = [S_{11}^{t\text{-}t}] + [S_{12}^{t\text{-}t}][\Lambda]\{[I] - [S_{22}^{t\text{-}t}][\Lambda]\}^{-1}[S_{21}^{t\text{-}t}] \tag{5}$$

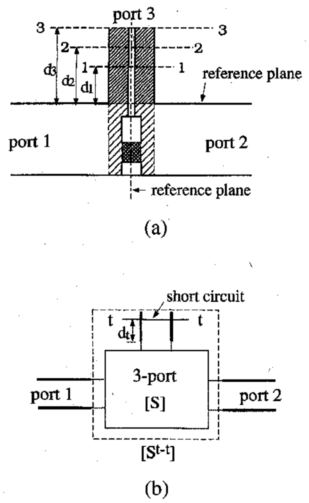

Fig. 2. (a) Coaxial-waveguide T-junction with coaxial port shorted at three different positions, and (b) S-matrix network representation.

where $[\Lambda]$ is a diagonal matrix with diagonal element $\Lambda_{ii} = -\exp^{-2\gamma_i^w \ell}$. γ_i^w is the propagation constant of ith waveguide mode. $[I]$ represents the identity matrix.

B. Extraction of S-Matrix

Assuming that there are $N_W^{(i)}$ $(i = 1, 2)$ modes in waveguide 'i' and that only the dominant TEM mode exists in the coaxial line beyond the position 1-1 (Fig. 2(a)), then the S-matrix of the T-junction has the following form

$$[S] = \begin{bmatrix} [S_{11}]_{N_W^{(1)} \times N_W^{(1)}} & [S_{12}]_{N_W^{(1)} \times N_W^{(2)}} & [S_{13}]_{N_W^{(1)} \times 1} \\ [S_{21}]_{N_W^{(2)} \times N_W^{(1)}} & [S_{22}]_{N_W^{(2)} \times N_W^{(2)}} & [S_{23}]_{N_W^{(2)} \times 1} \\ [S_{31}]_{1 \times N_W^{(1)}} & [S_{32}]_{1 \times N_W^{(2)}} & S_{33} \end{bmatrix}. \quad (6)$$

When the coaxial port is shorted at positions t-t $(t = 1, 2,$ and 3), the three-port S-matrix $[S]$ of the T-junction reduces to the two-port S-matrix $[S^{t\text{-}t}]$ of a general cylindrical post in a rectangular waveguide (Fig. 2(b)) solved in (3). The relationship between $[S]$ and $[S^{t\text{-}t}]$ can be readily obtained as

$$\left(\frac{1}{\Gamma_t} - S_{33}\right)[S_{ij}^{t\text{-}t}] = \left(\frac{1}{\Gamma_t} - S_{33}\right)[S_{ij}] + [S_{i3}][S_{3j}] \qquad i,\ j = 1, 2; \quad t = 1, 2, 3 \quad (7)$$

where $\Gamma_t = -e^{-j2\beta d_t}$. β is the propagation constant of TEM mode in the coaxial line.

From above equations, $[S]$ may be extracted as

$$S_{33} = \frac{1}{4}\left(S_{33}^{(11)} + S_{33}^{(12)} + S_{33}^{(21)} + S_{33}^{(22)}\right) \quad (8a)$$

$$[S_{ij}]_{\substack{i\neq 3\\ j\neq 3}} = \Gamma_1 \Delta_{21}\left(\frac{1}{\Gamma_1} - S_{33}\right)[S_{ij}^{1\text{-}1}] + \Gamma_2 \Delta_{12}\left(\frac{1}{\Gamma_2} - S_{33}\right)[S_{ij}^{2\text{-}2}] \quad (8b)$$

$$[S_{i3}][S_{3j}]_{\substack{i\neq 3\\ j\neq 3}} = \left(\frac{1}{\Gamma_1} - S_{33}\right)[S_{ij}^{1\text{-}1}] - \left(\frac{1}{\Gamma_1} - S_{33}\right)[S_{ij}] \quad (8c)$$

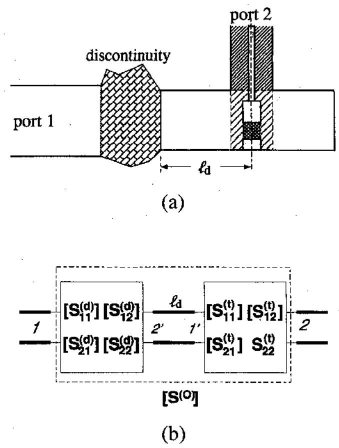

Fig. 3. (a) Coaxial-waveguide transition near a waveguide discontinuity, and (b) network representation of the cascaded structure.

with

$$S_{33}^{(pq)} = \frac{\Delta_{21}[S_{pq}^{1\text{-}1}]_{11} + (\Delta_{12} - \Delta_{32})[S_{pq}^{2\text{-}2}]_{11} - \Delta_{23}[S_{pq}^{3\text{-}3}]_{11}}{\Gamma_1\Delta_{21}[S_{pq}^{1\text{-}1}]_{11} + \Gamma_2(\Delta_{12} - \Delta_{32})[S_{pq}^{2\text{-}2}]_{11} - \Gamma_3\Delta_{23}[S_{pq}^{3\text{-}3}]_{11}} \quad (8d)$$

where $\Delta_{ij} = \frac{\Gamma_i}{\Gamma_i - \Gamma_j}$. The average taken in (8a) is used to minimize the error of the solution. When $N_W^{(1)} = N_W^{(2)}$, the properties of symmetrical networks can be applied to reduce the computational effort.

Similarly, the S-matrix of a transition has the form

$$[S] = \begin{bmatrix} [S_{11}]_{N_W^{(1)} \times N_W^{(1)}} & [S_{12}]_{N_W^{(1)} \times 1} \\ [S_{21}]_{1 \times N_W^{(1)}} & S_{22} \end{bmatrix}. \quad (9)$$

This 2-port S-matrix can be found either from the T-junction S-matrix by terminating waveguide port 2 at proper position or from three one-port reflection matrices $[R^{t\text{-}t}]$ $(t = 1, 2,$ and 3) obtained in the last section. No matter which method is used, one can only solve for $\{[S_{12}][S_{21}]\}$, but not for $[S_{12}]$ and $[S_{21}]$ separately. However, it will not effect the applications of the modeling in many practical cases as being discussed in the next section.

The accuracy of above extraction depends on the accuracy of the solution at each short plane. The selection of the short plane positions may also affect the accuracy of the extraction. The optimum choice of the positions of the three short planes is to make the phase difference between each two of them 120°.

C. Cascading Algorithm

In many applications, a coaxial probe is often placed in close proximity to a waveguide discontinuity. In this case, a modified cascading procedure can be applied as long as one can obtain the generalized scattering matrix of the discontinuity. The coaxial line to waveguide transition cascaded with a waveguide discontinuity through a length of waveguide is shown in Fig. 3. The S-matrices of the transition and discontinuity are $[S^{(t)}]$ and $[S^{(d)}]$, respectively. Because we

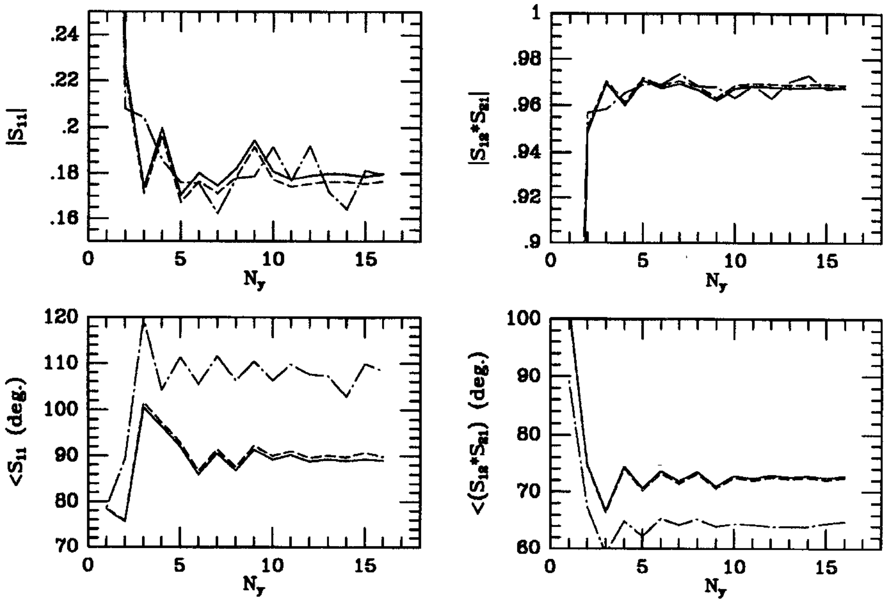

Fig. 4. Convergence of S-parameters of a coaxial-waveguide transition with a disc loaded probe with different N_x:— $N_x = 7$, ··· $N_x = 5$, - - - $N_x = 3$, – · –$N_x = 1$. $2a = 0.9''$, $b = 0.4''$, $r_0 = 0.025''$, $r_d = 0.045''$, $r_1 = 0.081''$, $b_1 = 0, b_2 = 0.2''$, $b_3 = 0.3''$, $\ell = 0.2''$, $\epsilon_{rd} = \epsilon_{rg} = 1.0$, $\epsilon_{rc} = 2.0$, and $f = 10$ GHz.

only know $\{[S_{12}^{(t)}][S_{21}^{(t)}]\}$, $[S_{12}^{(O)}]$ and $[S_{21}^{(O)}]$ of the overall structure can not be obtained separately. Instead, we have

$$[S_{11}^{(O)}] = [S_{11}^{(d)}] + [S_{12}^{(d)}]\{[I] - [\Gamma][S_{11}^{(t)}][\Gamma][S_{22}^{(d)}]\}^{-1} \times [\Gamma][S_{11}^{(t)}][\Gamma][S_{21}^{(d)}] \quad \text{(10a)}$$

$$[S_{12}^{(O)}][S_{21}^{(O)}] = [S_{12}^{(d)}]\{[I] - [\Gamma][S_{11}^{(t)}][\Gamma][S_{22}^{(d)}]\}^{-1}[\Gamma] \times \{[S_{12}^{(t)}][S_{21}^{(t)}]\} \times \{[I] - [\Gamma][S_{22}^{(d)}][\Gamma][S_{11}^{(t)}]\}^{-1}[\Gamma][S_{21}^{(d)}] \quad \text{(10b)}$$

$$S_{22}^{(O)} = S_{22}^{(t)} + [S_{21}^{(t)}][A][S_{12}^{(t)}] = S_{22}^{(t)} + \sum_{i=1}^{N_W^{(1)}}\sum_{j=1}^{N_W^{(1)}} a_{ij} \cdot (S_{21}^{(t)})_i (S_{12}^{(t)})_j \quad \text{(10c)}$$

with

$$[A] = \{[I] - [\Gamma][S_{22}^{(d)}][\Gamma][S_{11}^{(t)}]\}^{-1}[\Gamma][S_{22}^{(d)}][\Gamma] \quad \text{(10d)}$$

where $[\Gamma]$ is a diagonal matrix describing the length of the waveguide with diagonal elements given by $\Gamma_{i,i} = e^{-\gamma_i^w \ell_d}$. a_{ij} is element of matrix $[A]$; $(S_{21}^{(t)})_i$ is ith element of the row vector $[S_{21}^{(t)}]$; and $(S_{12}^{(t)})_j$ jth element of the column vector $[S_{12}^{(t)}]$.

Evaluation of 10(a) and (b) is straightforward if all submatrices of $[S^{(d)}]$ are known. One also has enough information to compute $S_{22}^{(O)}$ if one notices that $(S_{21}^{(t)})_i(S_{12}^{(t)})_j$ is the element in the jth row and ith column of the matrix $\{[S_{12}^{(t)}][S_{21}^{(t)}]\}$ which is known from the transition modeling.

III. Results

Computer programs have been developed to calculate the S-matrix of a coaxial-waveguide T-junction or a coaxial-waveguide transition. The eigenmodes used in waveguide regions and cylindrical region III are selected according to the rule given in Section II. The numbers of the modes in ϕ-variation in all cylindrical regions are the same, but the number of modes in y-variations in each region is determinated by the ratio of the region height to the height of region III in order to have good convergence. Numerical experiments show that the convergence changes with the complexity of the shape of the probe. Sample results showing the convergence of the S-parameters of the dominant modes for a coaxial-waveguide transition with a disc loaded probe are shown in Fig. 4. In this case, $N_x = 5$ and $N_y = 12$ provide a convergent result. For the probe with simple shape, $N_x = 5$ and $N_y = 10$ will be sufficient. The computation time depends on the numbers of the modes used. For the case of $N_x = 5$ and $N_y = 10$, it takes about one minute to obtain the scattering matrix of a T-junction or a transition at one frequency point on the Sun Station 5.

Fig. 5 shows the dominant mode scattering parameters of a coaxial-waveguide T-junction in which the dielectric coated coaxial probe is extended from the top to the bottom of the waveguide. f_c is the cut-off frequency of TE_{10} mode in the waveguide. The figure also shows the measured results of the S-parameters. The two sets of results are in excellent agreement.

Fig. 6 compares the computed and measured results of the dominant mode S-parameters for a coaxial-waveguide transition with a disc loaded probe. It can be seen that a good agreement between the numerical results and the experimental results is achieved. The return loss of an adaptor with a disc loaded probe is given in Fig. 7. Also included are the measured and simulated results by [18].

In Fig. 8, the input impedance $Z_{in} = R_{in} + jX_{in}$ at the coaxial port of a coaxial-waveguide transition with a tuning

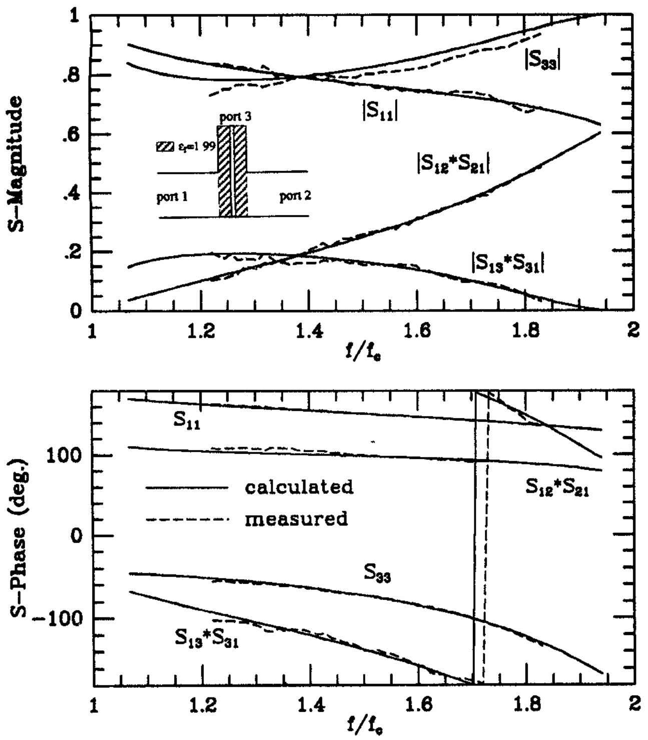

Fig. 5. Dominant mode S-parameters of a coaxial-waveguide T-junction with a dielectric coated probe with $b/2a = 0.4444$, $r_0/a = 0.0556$, and 50 Ω coaxial line.

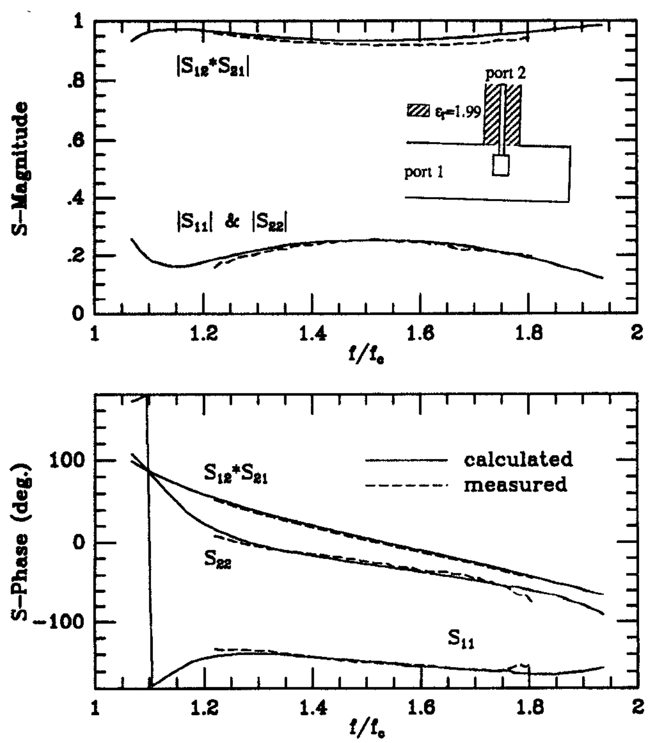

Fig. 6. Dominant mode S-parameters of a coaxial-waveguide transition with a disc loaded probe with $b/2a = 0.4444, b_1 = 0, b_2/b = 0.425$, $(b_3 - b_2)/b = 0.2975$, $\ell/2a = 0.3889, r_0/a = 0.0556$, $r_d/r_0 = 2.14$, and 50 Ω coaxial line.

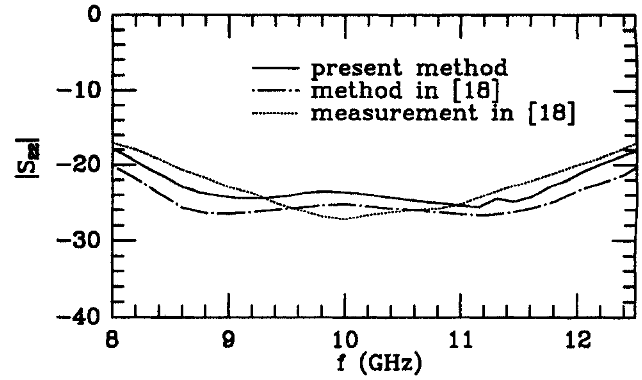

Fig. 7. Comparison between experimental and theoretical results for the return loss of an adaptor with a disc loaded probe with $2a = 0.9''$, $b = 0.4''$, $r_0 = 0.0256''$, $r_d = 0.0807''$, $\ell = 0.3228''$, $b_1 = 0$, $b_2 = 0.2071''$, $b_3 = 0.3094''$, $\epsilon_{rd} = \epsilon_{rg} = 1$, and a 50 Ω SMA connector.

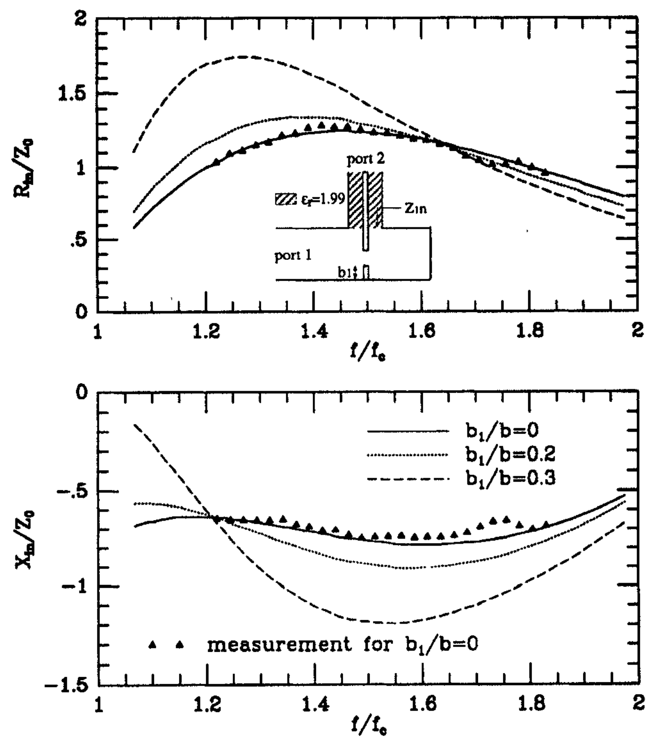

Fig. 8. Input impedance of a coaxial probe excited semi-infinite waveguide with a tuning rod from bottom wall of waveguide with $b/2a = 0.4444$, $b_2/b = 0.425$, $\ell/2a = 0.3889$, $r_0/a = 0.0556$.and 50 Ω coaxial line.

rod from the bottom wall is presented. The input impedance is normalized by the characteristic impedance of the coaxial line (Z_0) and computed from the reflection coefficient at the coaxial port (port 2 in this case). Also included are the measured results for $b_1 = 0$. Fig. 9 shows the input impedance at the coaxial port of a coaxial-waveguide T-junction versus the normalized frequency with change of the gap between the probe and the bottom wall. The results are extended to about $3.85f_c$. Beyond that, the modeling is no longer valid since the second propagating mode occurs in the coaxial line.

As an application of the modeling, the response of a probe-excited dielectric block filter [17] shown in Fig. 10 is simulated by cascading the probes with the dielectric block resonators coupled by empty evanescent mode waveguide. This filter is small in size and has an excellent stop band

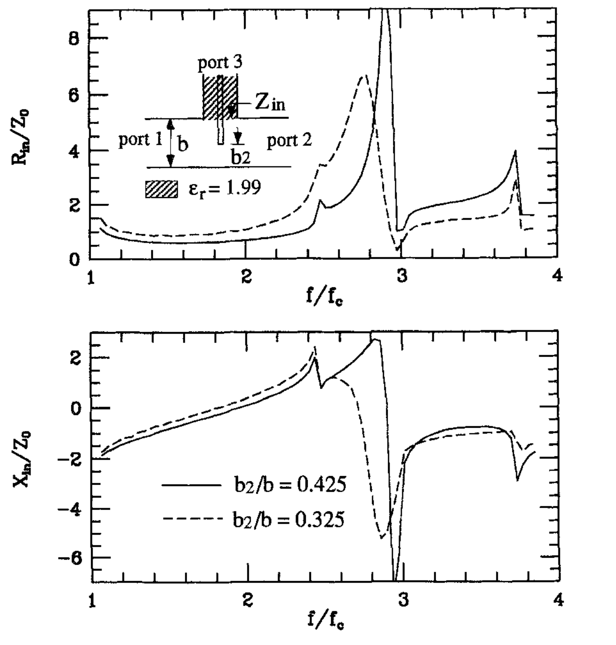

Fig. 9. Input impedance at the coax port of a coax-waveguide T-junction with $b/2a = 0.4444$, $b_1 = 0$, $r_0/a = 0.0556$, and 50 Ω coaxial line.

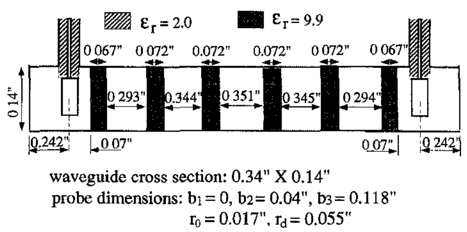

Fig. 10. Configuration of a probe-excited dielectric block filter with dimensions.

performance. The input/output probe is in the evanescent mode waveguide, and its dimensions was determined in [17] by experiments. The other dimensions shown in Fig. 10 are the measured values when the filter is partially assembled. The real dimensions, which are unknown, may differ from the given ones because of the way of assembling the filter to eliminate the air gaps. The simulated response of the filter with the dimensions given in Fig. 10 is presented and compared with the measured response in Fig. 11. As can be seen, fairly good agreement exists between numerical simulation and experiment. The variation of the return loss of the computed result is sharper than that of the measurement since the loss of the filter is not taken into account in the simulation.

IV. Conclusion

The paper describes a new rigorous approach, which combines the orthogonal expansion method and the extension of the three short plane technique, for analyzing a general coaxial probe in a rectangular waveguide. Scattering matrices are obtained for both coaxial-waveguide T-junctions and coaxial waveguide transitions. For solving the problem of a probe near a waveguide discontinuity, a cascading method is applied. As an application, the response of a probe-excited dielectric

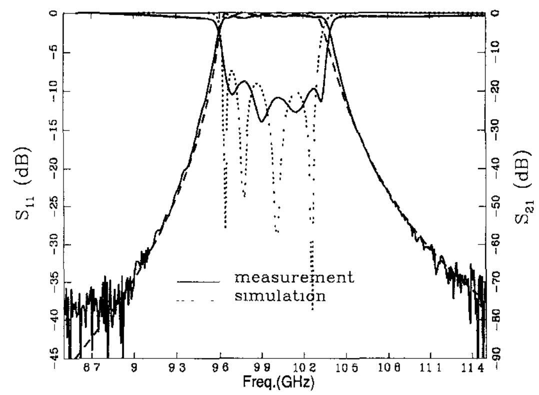

Fig. 11. Simulated and measured responses of the filter.

block filter is simulated. The computed results are in excellent agreement with the measured results for all cases. This method will be very useful in analysis and design of coaxial-waveguide adapters, coaxial probe excited cavity filters, and coaxial-waveguide T-junction manifold multiplexers.

References

[1] R. E. Collin, *Field Theory of Guided Waves*. New York: McGraw-Hill, 1960.

[2] A. G. Williamson, "Coaxially fed hollow probe in a rectangular waveguide," *Proc. Inst. Elec. Eng.*, 1985, vol. 132, Part H, pp. 273–285.

[3] J. M. Jarem, "A multifilament method-of-moments solution for the input impedance of a probe-excited semi-infinite waveguide," *IEEE Trans. Microwave Theory Tech.*, vol. MTT-35, pp. 14–19, Jan. 1987.

[4] M. E. Bialkowski, "Analysis of a coaxial-to-waveguide adaptor incorporating a dielectric coated probe," *IEEE Microwave and Guided Wave Lett.*, vol. 1, pp. 211–214, Aug. 1991.

[5] R. B. Keam and A. G. Williamson, "Analysis of a general coaxial-line/radial-line region junction," *IEEE Trans. Microwave Theory Tech.*, vol. 41, pp. 516–520, Mar. 1993.

[6] J.-F. Liang, H.-C. Chang, and K. A. Zaki, "Coaxial probe modeling in waveguides and cavities," *IEEE Trans. Microwave Theory Tech.*, vol. 40, pp. 2172–2180, Dec. 1992.

[7] R. Gesche and N. Löchel, "Scattering by a lossy dielectric cylinder in a rectangular waveguide," *IEEE Trans. Microwave Theory Tech.*, vol. 36, pp. 137–144, Jan. 1988.

[8] R. Gesche and N. Löchel, "Two cylindrical obstacles in a rectangular waveguide—Resonances and filter applications," *IEEE Trans. Microwave Theory Tech.*, vol. 37, pp. 962–968, June 1989.

[9] X.-P. Liang and K. A. Zaki, "Modeling of cylindrical dielectric resonators in rectangular waveguides and cavities," *IEEE Trans. Microwave Theory Tech.*, vol. 41, pp. 2174–2181, Dec 1993.

[10] Y. Y. Tsai and A. S. Omar, "Field theoretical treatment of E-plane waveguide junctions with anisotropic medium," *IEEE Trans. Microwave Theory Tech.*, vol. 40, pp. 2164–2171, Dec. 1992.

[11] M. Sucher and J. Fox, *Handbook of Microwave Measurements*, vol. 1. New York: Polytechnical Press, 1963.

[12] X.-P. Liang, K. A. Zaki, and A. E. Atia, "A rigorous three plane mode-matching technique for characterizing waveguide T-junctions, and its application in multiplexer design," *IEEE Trans. Microwave Theory Tech.*, vol. 39, pp. 2138–2147, Dec. 1991.

[13] H.-W. Yao, A. Abdelmonem, J.-F. Liang, X.-P. Liang, and K. A. Zaki, "Wide-band waveguide and ridge waveguide T-junctions for diplexer applications," *IEEE Trans. Microwave Theory Tech.*, vol. 41, pp. 2166–2173, Dec. 1993.

[14] S.-W. Chen and K. A. Zaki, "Dielectric ring resonators loaded in waveguide and on substrate," *IEEE Trans. Microwave Theory Tech.*, vol. MTT-39, pp. 2069–2076, Dec. 1991.

[15] R. Mittra and S. W. Lee, *Analytic Techniques in the Theory of Guided Waves*. New York: Macmillan, 1971.

[16] R. R. Mansour and R. H. MacPhie, "An improved transmission matrix formulation of cascaded discontinuities and its application to E-plane circuits," *IEEE Trans. Microwave Theory Tech.*, vol. MTT-34, pp. 1490–1498, Dec. 1986.

[17] A. Abdelmonem, J.-F. Liang, H.-W. Yao, and K. A. Zaki, "Spurious free D.R. TE mode band pass filter," in *IEEE MTT-S, Int. Microwave Symp. Dig.*, San Diego, CA, 1994, pp. 735–738.
[18] M. E. Bialkowski, "Analysis of a coaxial-to-waveguide adaptor including a discended probe and a tuning post," *IEEE Trans. Microwave Theory Tech.*, vol. 43, pp. 344–349, Feb. 1995.
[19] H.-W. Yao, K. A. Zaki, A. E. Atia, and R. Hershtig, "Full wave modeling of conducting posts in rectangular waveguides and its applications to slot coupled combline filters," *IEEE Trans. Microwave Theory Tech.*, vol. 43, no. 12, pp. 2824–2830, Dec. 1995.

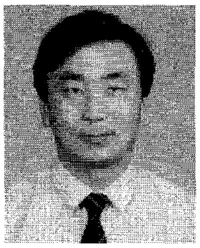

Hui-Wen Yao (S'92) was born in Inner Mongolia, China, in 1962. He received the B.S. and M.S. degrees, both in electrical engineering, from Beijing Institute of Technology, Beijing, China, in 1983 and 1986, respectively.

From 1986 to 1991, he was a Lecturer in the Department of electrical engineering, Beijing Institute of Technology, where his research dealt mainly with EM radiation, scattering and antenna design. From 1991 to 1992, he held the position of Teaching Assistant in Electrical Engineering Department, Wright State University, Dayton, Ohio, where he worked on microstrip circuits and transient scattering by cylinders. Presently, he is a Research Assistant in the Microwave Laboratory, Department of Electrical Engineering in UMCP, working toward the Ph.D. degree. His current research interests include analysis, modeling and design of microwave and millimeter-wave devices and circuits.

Kawthar A. Zaki (SM'85–F'91) received the B.S. degree with honors from Ain Shams University, Cairo, Egypt, in 1962, and the M.S. and Ph.D. degrees from the University of California, Berkeley, in 1966 and 1969, respectively, all in electrical engineering.

From 1962 to 1964, she was a Lecturer in the Department of Electrical Engineering, Ain Shams University. From 1965 to 1969, she held the position of Research Assistant in the Electronic Research Laboratory, University of California, Berkeley. She joined the Electrical Engineering Department, University of Maryland, College Park, MD, in 1970, where she is presently Professor of Electrical Engineering. Her research interests are in the areas of electromagnetics, microwave circuits, optimization, computer-aided design, and optically controlled microwave and millimeter wave devices.